Acta Crystallographica Section D
Biological Crystallography
ISSN 0907-4449

Structure of a d(TGGGGT) quadruplex crystallized in the presence of Li^+ ions

Christophe Creze,[a] Bruno Rinaldi,[b]‡ Richard Haser,[a] Philippe Bouvet[b] and Patrice Gouet[a]*

[a]Laboratoire de BioCristallographie, Institut de Biologie et Chimie des Protéines, CNRS–UCBL, UMR 5086 and IFR128 'BioSciences Lyon-Gerland', 7 Passage du Vercors, 69007 Lyon, France, and [b]Laboratoire de Biologie Moléculaire de la Cellule, Laboratoire Joliot-Curie, Ecole Normale Supérieure de Lyon, CNRS–UMR 5161, INRA 1237 and IFR128 'BioSciences Lyon-Gerland', 46 Allée d'Italie, 69007 Lyon, France

‡ Present address: Equipe 'Transcription: ciblage à vocation thérapeutique', Ecole Superieure de Biotechnologie de Strasbourg, UMR 7175, Boulevard Sébastien Brant, 67412 Illkirch, France.

Correspondence e-mail: p.gouet@ibcp.fr

Received 23 January 2007
Accepted 20 March 2007

PDB Reference:
5′-(TGGGGT)-3′ quadruplex, 2o4f, r2o4fsf.

A parallel 5′-d(TGGGGT)-3′ quadruplex was formed in Na^+ solution and crystallized using lithium sulfate as the main precipitating agent. The X-ray structure was determined to 1.5 Å resolution in space group $P2_1$ by molecular replacement. The asymmetric unit consists of a characteristic motif of two quadruplexes stacked at their 5′ ends. All nucleotides are clearly defined in the density and could be positioned. A single bound Li^+ ion is observed at the surface of the column formed by the two joined molecules. Thus, this small alkali metal ion appears to be unsuitable as a replacement for the Na^+ ion in the central channel of G-quartets, unlike K^+ or Tl^+ ions. A well conserved constellation of water molecules is observed in the grooves of the dimeric structure.

1. Introduction

Depending on their sequences, oligonucleotides can fold into various secondary structures *via* intramolecular or intermolecular interactions. DNA sequences containing runs of guanine-rich segments are widely dispersed in eukaryotic genomes and are of particular interest. Interest in them has grown in recent years because of their implication in many important cellular processes such as telomere maintenance (Perry *et al.*, 2001) and gene-transcription regulation (Cogoi *et al.*, 2004). These sequences can form unusual DNA structures called quadruplexes (Gilbert & Feigon, 1999; Shafer & Smirnov, 2000; Burge *et al.*, 2006) based on the association of guanines. These structures are also emerging as a new class of molecular targets (Hurley, 2001). G-quadruplexes are believed to be potential therapeutic targets for cancer (Cogoi & Xodo, 2006) and other diseases (Jing *et al.*, 2000; Hurley, 2001; Chou *et al.*, 2005; Ghosal & Muniyappa, 2006).

Intensive studies have been performed on the short DNA sequence 5′-d(TGGGGT)-3′ (Stefl *et al.*, 2003; Mergny *et al.*, 2005; Merkina & Fox, 2005) found in *Tetrahymena*. This guanine-rich segment self-assembles in the presence of Na^+ ions and forms parallel-stranded structures as shown by NMR studies (Aboul-ela *et al.*, 1992, 1994) and X-ray crystallography to 0.95 Å resolution (Laughlan *et al.*, 1994; Phillips *et al.*, 1997). Guanine bases display an *anti* conformation about the glycosidic bond, interact *via* Hoogsteen hydrogen bonding (Hoogsteen, 1963) and form tetrads. They are stacked on one another and organized around a central channel of Na^+ ions. These ions can be exchanged for Tl^+, as observed in two recent crystallographic structures determined to 2.2 and 2.5 Å resolution (Caceres *et al.*, 2004). Structural studies have also been performed on the equivalent guanine-rich RNA sequence

5′-(UGGGGU)-3′ in the presence of K^+ or Sr^{2+} ions (Cheong & Moore, 1992; Deng *et al.*, 2001). A parallel RNA quadruplex is formed with a similar geometry. However, uracils have a greater propensity to assemble in tetrads stacked over guanines tetrads than thymines. Parallel-stranded structures of DNA and RNA purine-rich segments containing both adenine and guanine tetrads have also been reported (Gavathiotis & Searle, 2003; Pan *et al.*, 2003). Longer guanine-rich segments tend to form antiparallel stranded structures with guanines in both *anti* and *syn* conformations. They are stabilized by a similar central channel of counterions as shown by Na^+, K^+ and NH_4^+-bound forms (Strahan *et al.*, 1998; Hud *et al.*, 1999; Schultze *et al.*, 1999). For an up-to-date review, see Burge *et al.* (2006).

Here, we report the 1.5 Å resolution structure of a 5′-d(TGGGGT)-3′ quadruplex crystallized in a monoclinic space group in the presence of Li^+ counterions. The molecular details of the model are analysed and the possibility of exchange between Na^+ and Li^+ ions in the central channel of the quadruplex is investigated.

2. Materials and methods

2.1. Oligonucleotide synthesis and purification

Oligonucleotides were purchased from Invitrogen as PCR primers and dissolved at 5.4 m*M* in 10 m*M* Tris–HCl pH 7.4 and 75 m*M* NaCl. Quadruplex formation was induced by heating for 5 min at 368 K followed by slow cooling to 277 K. The quadruplex was purified by gel filtration on a Superdex75 HR/10/30 column (GE Healthcare) on an ÄKTA Purifier (GE Healthcare) and was concentrated to 1.3 m*M* (quadruplex concentration) using a 5 kDa molecular-weight cutoff membrane (Vivascience).

2.2. Crystallization

Crystallization trials took place using commercial screens and the vapour-diffusion method at 277 and 292 K. Hanging drops were obtained by mixing 1 µl DNA solution and 1 µl crystallization solution and were equilibrated against a well containing 500 µl crystallization solution. Hampton Research Natrix Screen condition No. 12 (10 m*M* magnesium sulfate, 50 m*M* sodium cacodylate pH 6.0, 1.8 *M* lithium sulfate monohydrate) produced crystals of dimensions 0.2 × 0.2 × 0.05 mm within one week at 277 K. The crystals were multiple and required manual dissection. Screening around this condition did not yield better crystals, but showed the crystals to be temperature-sensitive. Crystals were cryoprotected by adding 0.5 µl ethylene glycol to the hanging drop. They were mounted at 277 K in a cryoloop and frozen in liquid nitrogen prior to data collection. Preliminary X-ray measurements were taken in-house on a MAR 345 Research image-plate system using Cu $K\alpha$ radiation from a Nonius 591 rotating-anode generator. The crystals belonged to space group $P2_1$, with unit-cell parameters a = 28.9, b = 57.4, c = 35.9 Å, β = 108.0°. The asymmetric unit contained two quadruplexes (Table 1). The calculated V_M value was 1.8 Å^3 Da^{-1}, which corresponds to a solvent content of 32% (Matthews, 1968).

Table 1
Data-collection and refinement statistics.

Values in parentheses are for the highest resolution shell.

Data-collection statistics	
Space group	$P2_1$
Unit-cell parameters (Å, °)	a = 28.9, b = 57.4, c = 35.9, β = 108.0
Wavelength (Å)	0.8726
Resolution range (Å)	15.0–1.5 (1.59–1.5)
No. of unique reflections	18195 (2977)
Overall redundancy	1.7 (1.7)
Completeness (%)	96.4 (93.4)
Mean $I/\sigma(I)$	7.1 (2.7)
R_{sym}	9.9 (22.7)
Refinement statistics	
Work/test reflections	17319/851
R_{work}/R_{free} (%)	20.4/25.7
Asymmetric unit content	Two quadruplexes
DNA atoms	1000
Na^+ ions	7
Li^+ ions	1
Water molecules	228
R.m.s.d. bonds (Å)	0.013
R.m.s.d. angles (°)	1.60
Mean temperature factor (Å^2)	
DNA	9.93
Ions	5.86
Waters	26.9

2.3. Data collection and processing

A data set was collected to 1.5 Å resolution at the ID23-2 beamline at ESRF, Grenoble, France. The crystal-to-detector distance was 168 mm, the oscillation step 1°, the total oscillation range 80° and the wavelength 0.8726 Å. Data were processed with *XDS* (Kabsch, 1993). They were merged, scaled and reduced with *XSCALE* (Kabsch, 1993). The systematic reflection condition 0k0: $k = 2n$ clearly confirmed that the space group was $P2_1$. Statistics are presented in Table 1. The structure was solved by molecular replacement using the program *AMoRe* (Navaza, 2001) and a two-body search based on a single quadruplex extracted from the 0.95 Å high-resolution structure (Phillips *et al.*, 1997) available from the Protein Data Bank (Berman *et al.*, 2000) under the code 352d. The initial R factor was 34% to 2.5 Å resolution.

Crystallographic refinement was performed with *CNS* (Brünger *et al.*, 1998) against all data to 1.5 Å resolution. The free R factor (Brünger, 1992) was calculated on 5% of the reflections and was monitored throughout all stages of refinement. The first calculated Fourier $2F_o - F_c$ electron-density maps were of excellent quality. Moreover, the thymines that were disordered in the 352d model appeared to be perfectly ordered in the present structure. Manual corrections were performed with the graphics software package *TURBO-FRODO* (Roussel & Cambillau, 1989). Finally, all nucleotide residues could be positioned and the structure was refined to an R factor of 20.4% (Table 1).

The present model is made up of eight strands named *A*–*H*. It contains 1000 DNA non-H atoms (two quadruplexes), seven

Na^+ ions, one Li^+ ion and 228 water molecules. Analyses of the conformation of the DNA sequences were performed using *CURVES* (Lavery & Sklenar, 1989) and the classical definitions and nomenclature of nucleic acid structure components (Dickerson, 1989). Structure superimpositions were carried out using *LSQKAB* (Kabsch, 1976). Images were generated using *DS Visualizer* (Accelrys Inc.) and *BobScript* (Esnouf, 1999).

3. Results

3.1. Crystal packing

The two quadruplexes present in the asymmetric unit assemble in a dimer. They are coaxially stacked at their 5′-ends and resemble a column. Adjacent dimers pile up at their 3′-ends, but with a lateral translation between their axes of about 7.5 Å along the *a* axis (Fig. 1). As a consequence, regular pavements of dimeric quadruplexes parallel to the *ac* plane can be observed within the crystal lattice. Thymines at the 5′- and 3′-ends mediate lateral and longitudinal crystallographic contacts, as will be described later.

3.2. The guanine quartets

Each DNA strand follows a right-handed helical trajectory. A stack of eight tetrads of guanines ensure the framework of a dimer. In each tetrad, guanine bases assemble *via* Hoogsteen hydrogen bonding, are in the *anti* conformation and respect a fourfold rotation symmetry along the helix axis (Fig. 2). The guanine tetrads are rotated with respect to each other within the quadruplex and with a helical rise of about 3.4 Å. The 5′–5′ dimeric interface is formed by the stacking of the first guanine tetrads of each molecule. The two tetrads overlap back to back *via* their five-membered rings. It can be noticed that the 5′-d(TGGGGT)-3′ NMR structure is constituted of a single quadruplex (Aboul-ela *et al.*, 1994), whereas the formation of dimeric quadruplexes is inherent to crystallographic structures. Thus, identical features have been reported in (i) the high-resolution structure 352d solved with two dimeric quadruplexes in the asymmetric unit (Phillips *et al.*, 1997), (ii) the Tl^+-bound structure 1s45 with one dimer and (iii) the Tl^+-bound structure 1s47 with one dimer and one monomer that exhibits a unique thymine tetrad (Caceres *et al.*, 2004).

However, we observe in the present dimeric quadruplex that only four guanine planes belonging to the same tetrad are coplanar. The others are tilted with respect to the column axis and point toward the direction of the 5′-end junction (Fig. 3). Such a difference between the sets of guanine tetrads is also observed in the Tl^+-bound structure 1s45, but is less apparent in the high-resolution structure 352d. As a result, superimposition of all 5′-d(GGGG)-3′ atoms of the present dimer on those of 1s45 and 352d yields r.m.s. deviations of 0.4 and 0.7 Å, respectively.

3.3. 3′-End thymines at both noncrystallographic and crystallographic interfaces

The guanine tetrad that breaks the dyad symmetry belongs to the 5′–5′ interface (Fig. 3). Its linked sugar rings are in a C3′-*endo* puckering mode instead of the C2′-*endo* mode observed in the rest of the dimer. Moreover, its phosphate groups display an unusual conformation in the quadruplex with torsion angles α, β, γ that are *gauche*$^-$, *trans*, *gauche*$^+$ (Fig. 4). As a consequence, the 5′-end thymines preceding this unique tetrad are flipped out and protrude from the column (Fig. 5). The two atoms O2 and O4 of each base are in contact with water molecules. Lateral crystallographic interactions are ensured by the N3 atom of one base, which donates a hydrogen to a phosphate group of an adjacent hexanucleotide,

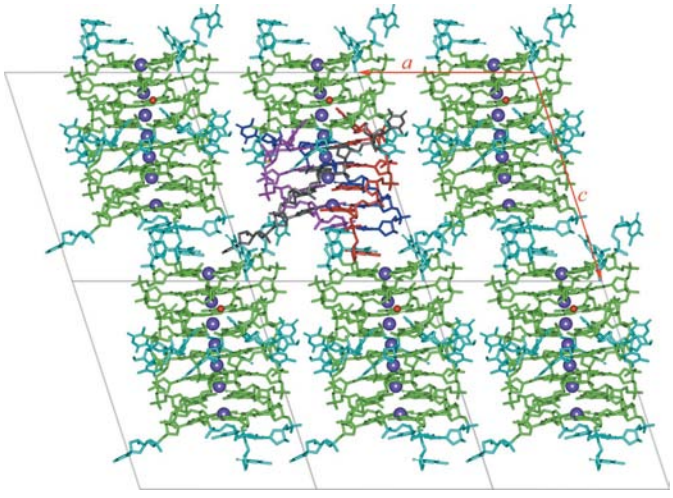

Figure 1
View of the crystal packing down the *b* axis. Thymines are coloured blue and guanines green. For clarity, strands are coloured differently in one quadruplex. Na^+ and Li^+ ions are shown as violet and red balls, respectively. Parallel columns form layers in the plane of the paper.

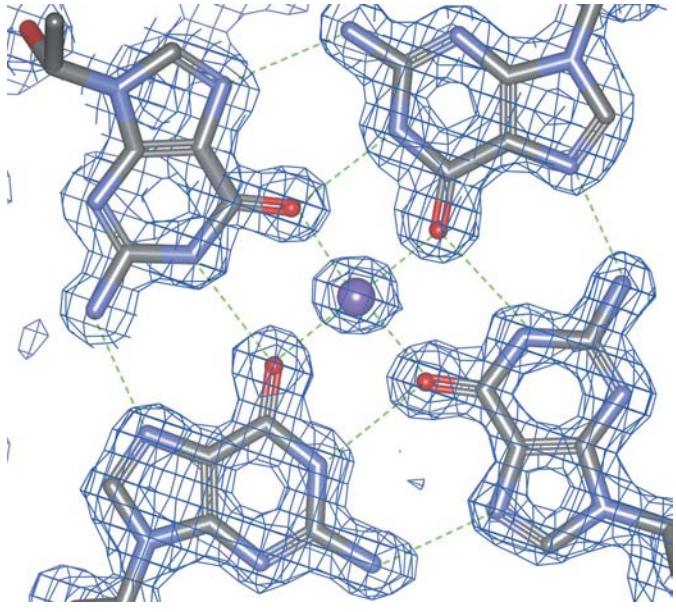

Figure 2
Representative electron-density view of a guanine tetrad. The $2F_o - F_c$ map is contoured at 1σ. The Na^+ ion is rendered as a violet ball. This ion is coordinated to the O6 atoms of the guanines.

and by a stacking between another 5′-end thymine and a 3′-end thymine of a neighbouring molecule.

The 5′-end thymines of the second molecule lean on the grooves of the first molecule (Fig. 5) and their O2 atoms are hydrogen bonded to the N2 atoms of the untilted guanines. A comparable arrangement of four purines and pyrimidines is observed in short RNA quadruplexes and is termed an octad (Deng *et al.*, 2001; Pan *et al.*, 2003). All 5′-thymines of the present structure are in the glycosidic *anti* conformation and respect the local fourfold rotational symmetry. Similar features are observed in the 1s45 structure (Caceres *et al.*, 2004), whilst the set of exposed thymines is more disordered in 1s47 and 352d, and does not obey fourfold symmetry.

3.4. 3′-End thymines at crystallographic interfaces

The 3′-end thymines also adopt an *anti* conformation. One triad of 3′-end thymines is stacked over the last guanine tetrad at each extremity of the dimer (Fig. 6*a*). The six-membered rings of the purine and pyrimidine bases overlap well in this peculiar stacking. Each triad includes at least one base of a crystallographically related molecule involved in an asymmetric double hydrogen bonding N3···O4, O2···N3 (Figs. 6*b* and 6*c*). Such a stable interaction between two pyrimidine bases favours longitudinal assembly of the crystal lattice, but prevents the formation of thymine tetrads. The strength of the crystal packing in the present structure is further ensured by a single face-to-face stacking of two thymines from different asymmetric unit at the 3′–3′ interface. Similar features of 3′-end thymines have been reported in equivalent parallel-stranded crystallographic structures (Phillips *et al.*, 1997; Deng *et al.*, 2001; Caceres *et al.*, 2004).

3.5. Monovalent counterions

A spine of seven Na^+ ions coincident with the fourfold-symmetry axis completes the stabilization of the dimeric quadruplex. One Na^+ ion is positioned at the centre of the 5′–5′ interface and coordinates eight O6 atoms of the surrounding tetrads. The six other Na^+ ions lie in symmetry in each quadruplex (Fig. 3). Thus, running from the 5′ to 3′ guanine tetrads, one ion is nearly equidistant between two tetrads, one is displaced toward the 3′-end but still sandwiched between two guanine tetrads and one lies within the planes of the 3′-terminal tetrad and is coordinated to four O6 atoms and one water molecule. The latter water lies along the helix axis, is connected to two O4 atoms of the thymine triad and caps the central channel. An identical arrangement of counterions and of capping water molecules is reported in the high-resolution structure 352d (Phillips *et al.*, 1997), whereas Na^+

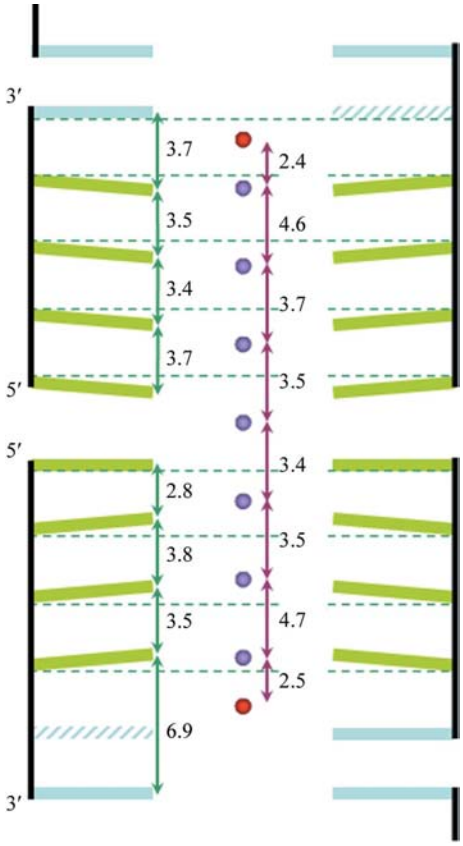

Figure 3
Schematic view of two adjacent quadruplexes showing the separation of the guanine tetrads and of Na^+ ions. The upper quadruplex is made up of strands *A*, *B*, *C* and *D*. The lower quadruplex contains strands *E*, *F*, *G* and *H* and the guanine tetrads at the 5′ extremity that break the dyad symmetry. Guanines are rendered as green rectangles, thymines as blue rectangles and thymines of the adjacent quadruplex as striped blue rectangles. Na^+ ions are pictured as violet balls. The two capping water molecules are shown as red balls. Distances are in Å.

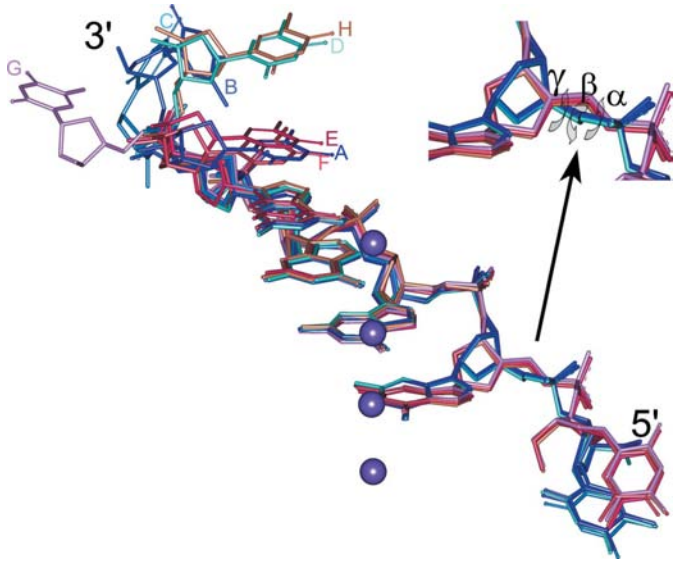

Figure 4
Superimposition of the eight strands of two neighbouring quadruplexes. Strands *ABCD* are shown in shades of blue and green. Strands *EFGH* have flipped-out thymines and are coloured in shades of red. Na^+ ions lie along the axes of the quadruplex and are pictured as violet balls. Note the geometry of the 5′-end thymine: for molecules *A*, *B*, *C* and *D* the torsion angles P—O5′ (α), O5′—C5′ (β) and C5′—C4′ (γ) are *gauche*$^-$ ($300 \pm 3^\circ$), *trans* ($193 \pm 4^\circ$) and *gauche*$^+$ ($53 \pm 3^\circ$), respectively. For molecules *E*, *F*, *G* and *H*, they are *gauche*$^+$ ($70 \pm 5^\circ$), *trans* ($175 \pm 4^\circ$) and *trans* ($169 \pm 8^\circ$), respectively. Guanine has the 'classical' angles *gauche*$^-$ ($296 \pm 10^\circ$), *trans* ($189 \pm 15^\circ$) and *gauche*$^+$ ($49 \pm 8^\circ$), respectively.

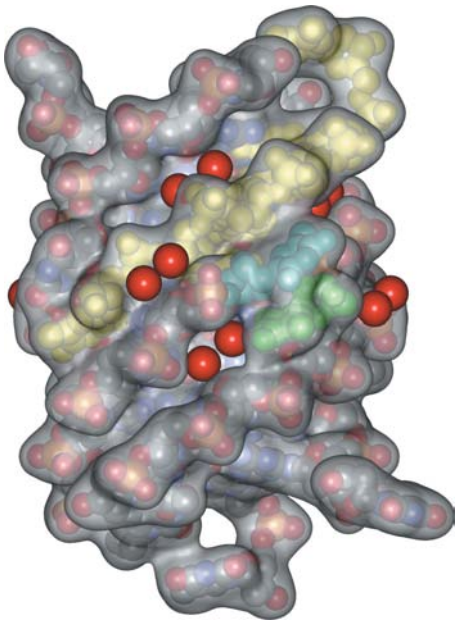

Figure 5
Localization of conserved water molecules on the molecular surface of the two quadruplexes. Only water molecules whose position is separated by less than 0.5 Å from symmetrical molecules generated by application of the local fourfold rotation symmetry are shown. They are pictured as red balls. To improve clarity, two stacked thymines are highlighted: the 5′-end thymines of the *C* strand (upper quadruplex) and the *E* strand (lower quadruplex) are coloured green and blue, respectively. The *D* strand is shown in yellow.

ions are partially exchanged for Tl^+ ions in 1s45 and in 1s47. Interestingly, the occupancy of the Tl^+ ions in 1s45 is much higher at the centre of the dimer than at the 3′ extremities and all counterions are located between guanine tetrads in 1s47. These results are consistent with the assumption that large counterions such as K^+, NH_4^+ and Tl^+ cannot fit within guanine tetrads because of steric hindrance (Hud *et al.*, 1996, 1999; Schultze *et al.*, 1999; Horvath & Schultz, 2001). In contrast, Li^+ ions are present at a molar concentration in the present crystallization solution and the question arises whether exchange of Na^+ for the smaller alkali metal may have occurred at both 3′-ends.

Li^+ is a weak scatterer and can clearly be distinguished from Na^+ in density. The two outer Na^+ ions of the dimeric quadruplex have individual temperature factors of 7 and 12 $Å^2$. In comparison, the five inner Na^+ ions and the two capping water molecules have temperature factors in the range 3–7 $Å^2$. Such low values rule out the hypothesis of any significant substitution. A single Li^+ ion is observed at the surface of the quadruplex column (Fig. 6). The geometry of the phosphate backbone is not modified at this position. It is coordinated to the sugar group of a guanine and to three water molecules (Fig. 7). We refined this species as Li^+, NH_4^+, Na^+ and water. Both R_{free} and *B*-factor values favoured Li^+, although not conclusively, but the tetrahedral environment and average coordination differences of 1.9 Å strongly support its identity as Li^+.

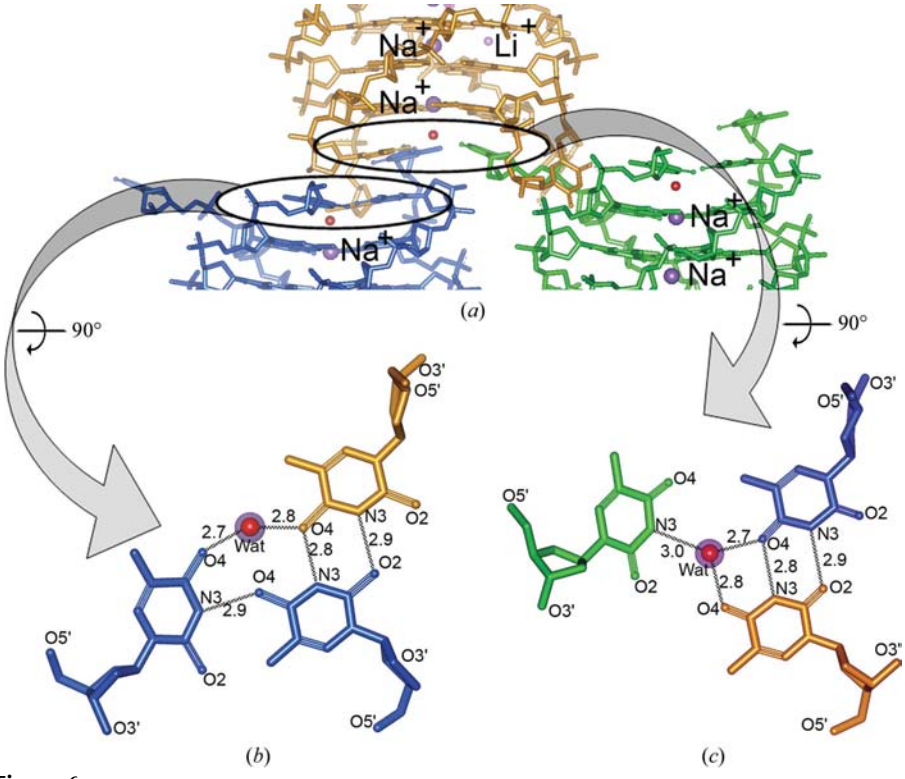

Figure 6
5′-end contacts between quadruplexes. (*a*) View along the central channel filled with Na^+ ions. (*b*) Enlargement of the triad involving two thymines of the lower quadruplex and one of the upper quadruplex. (*c*) Enlargement of the triad involving thymines from three neighbouring quadruplexes. Na^+ ions, Li^+ ion and water molecules are shown as large violet, small violet and red balls, respectively.

3.6. Hydration pattern

Water molecules are also important for the stability of the quadruplexes (Phillips *et al.*, 1997; Horvath & Schultz, 2001). They are well defined in the present 1.5 Å resolution structure and we have superposed the four stands of each DNA molecule to see whether their positions respect the fourfold symmetry. Most of the conserved water molecules lie deep inside the four equivalent grooves of the two quadruplexes as in 352d (Phillips *et al.*, 1997) (Fig. 5). There, they can bridge two parallel strands. Thus, a repeated water molecule is connected on the one side of the wall groove to the N3 atom of a guanine and the O4′ atom of a sugar ring and interacts on the other side with the O2P atom of a phosphate group.

4. Discussion

Our first crystallization trials were carried out with a protein–DNA complex. The studied protein, a human nucleolin, had been shown to interact with various G-quartet sequences *via*

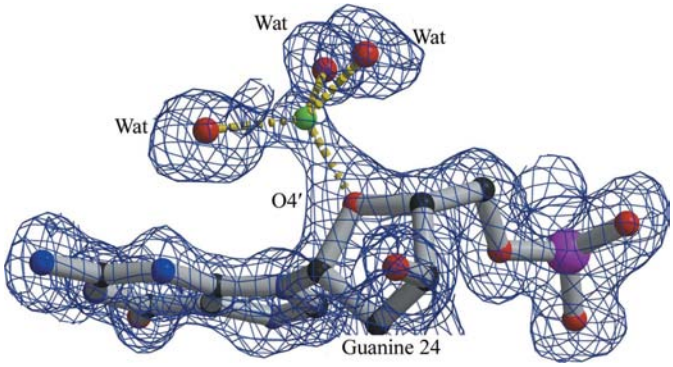

Figure 7
Electron-density view of the Li^+ ion. This ion (pictured as a green ball) coordinates three water molecules and the O4′ atom of the sugar group of a guanine. Distances are in the range 2.0–1.9 Å and the mean angle value is 109°. These values obey the ideal geometry of the lithium ion (Pye *et al.*, 2005). The $2F_o - F_c$ map is contoured at 1σ.

band-shift experiments (unpublished results; Hanakahi *et al.*, 1999). However, we only succeeded in growing DNA crystals. Previous authors have reported similar difficulties in crystallizing protein–quadruplex complexes (Caceres *et al.*, 2004) and only a few structures of crystallographic complexes involving G-quartets have been published (Horvath & Schultz, 2001; Clark *et al.*, 2003; Haider *et al.*, 2003).

Our crystallization solution contains a large quantity of Li^+ ions (1.8 *M* in the well solution), but no substitution of Na^+ ions has been detected in the core of the quadruplexes. This result can be explained by the low affinity of Li^+ ions in the central channel as reported previously (Wong & Wu, 2003). The reservoir solution also contained 10 m*M* $MgCl_2$. However, no bound divalent ions are observed in the present structure, whereas a single Mg^{2+} ion is located at the surface of a quadruplex in 1s45 and four Ca^{2+} ions lie at the periphery of the 5′–5′ interface in 352d. However, in both cases the concentration of divalent ion was sixfold to sevenfold higher. It can also be noticed that those bound counterions are mainly coordinated to water molecules, like Li^+ in the reported structure. They neither interact with two DNA atoms nor seem to have a strong impact on the quadruplex topology.

Thus, our results confirm that the 5′-d(TGGGT)-3′ quadruplex has a strong tendency to form dimers that are assembled head-to-head in different crystallization conditions: in the presence of $LiSO_4$ here, of NaCl and MPD in 352d (Phillips *et al.*, 1997), of MPD in 1s45 (Caceres *et al.*, 2004) and of PEG 400 in 1s47 (Caceres *et al.*, 2004). The present structure and that of 1s45 share the same asymmetrical 5′–5′ interface and can be superimposed with an r.m.s. deviation of 1 Å on all purine and pyrimidine atoms. The largest differences occur at the 3′-end thymines. These bases display various orientations and their assembly into tetrads is hindered by the formation of the crystal lattice.

This work was supported by a grant from the Region Rhône-Alpes, Action Cancer. The authors would like to thank Dr Xavier Robert for helpful comments in data processing and in figure preparation.

References

Aboul-ela, F., Murchie, A. I. & Lilley, D. M. (1992). *Nature (London)*, **360**, 280–282.
Aboul-ela, F., Murchie, A. I., Norman, D. G. & Lilley, D. M. (1994). *J. Mol. Biol.* **243**, 458–471.
Berman, H. M., Westbrook, J., Feng, Z., Gilliland, G., Bhat, T. N., Weissig, H., Shindyalov, I. N. & Bourne, P. E. (2000). *Nucleic Acids Res.* **28**, 235–242.
Brünger, A. T. (1992). *Nature (London)*, **355**, 472–475.
Brünger, A. T., Adams, P. D., Clore, G. M., DeLano, W. L., Gros, P., Grosse-Kunstleve, R. W., Jiang, J.-S., Kuszewski, J., Nilges, M., Pannu, N. S., Read, R. J., Rice, L. M., Simonson, T. & Warren, G. L. (1998). *Acta Cryst.* D**54**, 905–921.
Burge, S., Parkinson, G. N., Hazel, P., Todd, A. K. & Neidle, S. (2006). *Nucleic Acids Res.* **34**, 5402–5415.
Caceres, C., Wright, G., Gouyette, C., Parkinson, G. & Subirana, J. A. (2004). *Nucleic Acids Res.* **32**, 1097–1102.
Cheong, C. & Moore, P. B. (1992). *Biochemistry*, **31**, 8406–8414.
Chou, S. H., Chin, K. H. & Wang, A. H. (2005). *Trends Biochem. Sci.* **30**, 231–234.
Clark, G. R., Pytel, P. D., Squire, C. J. & Neidle, S. (2003). *J. Am. Chem. Soc.* **125**, 4066–4067.
Cogoi, S., Quadrifoglio, F. & Xodo, L. E. (2004). *Biochemistry*, **43**, 2512–2523.
Cogoi, S. & Xodo, L. E. (2006). *Nucleic Acids Res.* **34**, 2536–2549.
Deng, J., Xiong, Y. & Sundaralingam, M. (2001). *Proc. Natl Acad. Sci. USA*, **98**, 13665–13670.
Dickerson, R. E. (1989). *Nucleic Acids Res.* **17**, 1797–1803.
Esnouf, R. M. (1999). *Acta Cryst.* D**55**, 938–940.
Gavathiotis, E. & Searle, M. S. (2003). *Org. Biomol. Chem.* **1**, 1650–1656.
Ghosal, G. & Muniyappa, K. (2006). *Biochem. Biophys. Res. Commun.* **343**, 1–7.
Gilbert, D. E. & Feigon, J. (1999). *Curr. Opin. Struct. Biol.* **9**, 305–314.
Haider, S. M., Parkinson, G. N. & Neidle, S. (2003). *J. Mol. Biol.* **326**, 117–125.
Hanakahi, L. A., Sun, H. & Maizels, N. (1999). *J. Biol. Chem.* **274**, 15908–15912.
Hoogsteen, K. (1963). *Acta Cryst.* **16**, 907–916.
Horvath, M. P. & Schultz, S. C. (2001). *J. Mol. Biol.* **310**, 367–377.
Hud, N. V., Schultze, P., Sklenar, V. & Feigon, J. (1999). *J. Mol. Biol.* **285**, 233–243.
Hud, N. V., Smith, F. W., Anet, F. A. & Feigon, J. (1996). *Biochemistry*, **35**, 15383–15390.
Hurley, L. H. (2001). *Biochem. Soc. Trans.* **29**, 692–696.
Jing, N., Marchand, C., Liu, J., Mitra, R., Hogan, M. E. & Pommier, Y. (2000). *J. Biol. Chem.* **275**, 21460–21467.
Kabsch, W. (1976). *Acta Cryst.* A**32**, 922–923.
Kabsch, W. (1993). *J. Appl. Cryst.* **26**, 795–800.
Laughlan, G., Murchie, A. I., Norman, D. G., Moore, M. H., Moody, P. C., Lilley, D. M. & Luisi, B. (1994). *Science*, **265**, 520–524.
Lavery, R. & Sklenar, H. (1989). *J. Biomol. Struct. Dyn.* **6**, 655–667.
Matthews, B. W. (1968). *J. Mol. Biol.* **33**, 491–497.
Mergny, J. L., De Cian, A., Ghelab, A., Sacca, B. & Lacroix, L. (2005). *Nucleic Acids Res.* **33**, 81–94.
Merkina, E. E. & Fox, K. R. (2005). *Biophys. J.* **89**, 365–373.
Navaza, J. (2001). *Acta Cryst.* D**57**, 1367–1372.
Pan, B., Xiong, Y., Shi, K., Deng, J. & Sundaralingam, M. (2003). *Structure*, **11**, 815–823.
Perry, P. J., Arnold, J. R. & Jenkins, T. C. (2001). *Exp. Opin. Invest. Drugs*, **10**, 2141–2156.
Phillips, K., Dauter, Z., Murchie, A. I., Lilley, D. M. & Luisi, B. (1997). *J. Mol. Biol.* **273**, 171–182.

Pye, C. C., Tomney, M. R. & Enright, T. G. (2005). *Can. J. Anal. Sci. Spectrosc.* **50**, 254–263.
Roussel, A. & Cambillau, C. (1989). *TURBO-FRODO.* Silicon Graphics, Mountain View, CA, USA.
Schultze, P., Hud, N. V., Smith, F. W. & Feigon, J. (1999). *Nucleic Acids Res.* **27**, 3018–3028.
Shafer, R. H. & Smirnov, I. (2000). *Biopolymers*, **56**, 209–227.
Stefl, R., Cheatham, T. E. III, Spackova, N., Fadrna, E., Berger, I., Koca, J. & Sponer, J. (2003). *Biophys. J.* **85**, 1787–1804.
Strahan, G. D., Keniry, M. A. & Shafer, R. H. (1998). *Biophys. J.* **75**, 968–981.
Wong, A. & Wu, G. (2003). *J. Am. Chem. Soc.* **125**, 13895–13905.